PCCP

PAPER

View Article Online
View Journal | View Issue

Cite this: *Phys. Chem. Chem. Phys.*, 2018, **20**, 1716

Slow rheological mode in glycerol and glycerol–water mixtures

M. H. Jensen,[ab] C. Gainaru,[c] C. Alba-Simionesco,[b] T. Hecksher *[a] and K. Niss [a]

Received 21st September 2017,
Accepted 12th December 2017

DOI: 10.1039/c7cp06482a

rsc.li/pccp

Glycerol–water mixtures were studied at molar concentrations ranging from x_{gly} = 1 (neat glycerol) to x_{gly} = 0.3 using shear mechanical spectroscopy. We observed a low frequency mode in neat glycerol, similar to what has been reported for monohydroxy alcohols. This mode has no dielectric counterpart and disappears with increased water concentration. We propose that the hydrogen-bonded network formed between glycerol molecules is responsible for the observed slow mode and that water acts as a plasticizer for the overall dynamics and as a lubricant softening the hydrogen-bonding contribution to the macroscopic viscosity of this binary system.

I. Introduction

Hydrogen bonds play an important role in biology as well as technology. They govern the chemical and physical properties of bulk water, alcohols and sugars,[1–3] they play a central role in protein and DNA structures as well as being central in water interactions in other materials.[4] For this reason there is intense scientific focus on understanding the hydrogen bonds. Glycerol (propane-1,2,3-triol) is a small molecule with three hydroxyl groups which supports the forming of a 3D hydrogen-bonded network penetrating the bulk liquid. It is the most used liquid in fundamental studies of glassy dynamics, *e.g.* ref. 5–10, as well as being widely used in technology, notably due to its cryoprotectant properties[11–13] which are intimately connected to its large affinity to form hydrogen bonds. In this respect it is important to gain an understanding of the interaction between the glycerol hydrogen-bonded network and water not only from a fundamental point of view but also for unraveling the mechanisms behind the antifreezing effect of glycerol.[14,15]

Hydrogen-bonded molecules inherently comprise atoms with large electronegativity contrast and thus exhibit large electric polarizability, meaning that they have a strong signal in dielectric spectroscopy (DS). DS has therefore been widely used to study the dynamics of hydrogen-bonded liquids particularly in the supercooled regime. The dielectric properties of glycerol have been studied in an extremely broad dynamic range[16] and from its boiling point down to cryogenic temperatures.[17] In the supercooled regime its dielectric loss spectra are dominated by the structural relaxation process which can be fitted very well by single-peak functions. In this respect glycerol resembles the behavior of non-associated, van der Waals liquids. Glycerol–water mixtures are also extensively studied with DS[14,18–22] and also in this case the dielectric signal show no obvious signature of the hydrogen bonding association.

On the other hand, many alcohols with a single hydroxyl group per molecule (monoalcohols) display a much more complex dielectric pattern including an absorption mode which is slower than the structural relaxation, the so-called Debye process.[23–25] Currently there is a widespread contention that the Debye dynamics in monoalcohols is related to the formation of hydrogen-bonded supramolecular structures of polar short chains which for certain systems can be converted to non-polar rings at temperatures well above the glass transition temperature T_g, as illustrated by the temperature dependence of the Kirkwood correlation factor.[26] The hydrogen-bonded structures can also give rise to an additional peak in the static structure factor at low Q-vectors,[65] although the reverse is not true, a prepeak in the structure factor is not systematically associated with a slower than structural relaxation feature in the dynamics.[27,28] The family of liquids displaying a dielectric Debye process[29] includes, besides monoalcohols, secondary amides,[30] protic ionic liquids,[31] and several pharmaceuticals.[32,33]

The Debye process was for a long time considered merely a dielectric feature.[34] Recent rheology shear[35] and bulk modulus[36] studies, however, have demonstrated otherwise: low molecular weight monoalcohols exhibit slower-than-structural-relaxation dynamics commonly considered specific to covalently bonded structures. For polymeric melts it is well established that the entropic elasticity of covalently bonded structures leads to the emergence of slow mechanical modes which govern their steady-state viscosity and implicitly their macroscopic flow.[37]

Such polymer-like mechanical dynamics was mainly discussed in literature for monoalcohols, but more recent investigations

[a] *Glass & Time, IMFUFA, Department of Science and Environment, Roskilde University, P.O. Box 260, DK-4000 Roskilde, Denmark. E-mail: tihe@ruc.dk*
[b] *Laboratoire Léon Brillouin, CNRS CEA-UMR 12, CEA Saclay, 91191 Gif-sur-Yvette Cedex, France*
[c] *Fakultät Physik, Technische Universität Dortmund, 44221 Dortmund, Germany*

have also discovered it in an amine system.[38] Important for the present context is that although amine systems are also able to sustain hydrogen bonds, the slow rheology process was found to not have a dielectric counterpart, contrary to the situation for monoalcohols. Similar low-frequency mechanical and dielectric modes have also been reported for a family of ionic liquids in a study where the link between the slower-than-structural-relaxation dynamics and mesoscopic structure is made more directly.[39]

The systematic of the separation between Debye and alpha process seen in dielectrics is apparently conserved in the rheological signal for some systems[35,36] while the correlation is less clear in a study of the *N*-methyl-3-heptanol series (N = 2–6).[40] These observations suggest that mechanical spectroscopy is a important complementary technique which can offer a different perspective regarding the dynamical signatures of hydrogen-bonded structures in liquids.

To our knowledge this type of slow mechanical mode has not so far been identified in polyalcohols. In this paper we present data on glycerol and glycerol rich glycerol–water mixtures obtained with broadband shear mechanical spectroscopy revealing a slow contribution to the spectral density, which we interpret as a signature of the dynamics of the hydrogen-bonded network. The strength of this slow mode decreases with increasing the water content and virtually disappears at equimolar composition, x_{gly} = 0.5, corresponding to 20 volume percent of water. This would imply that water significantly changes the properties of the glycerol hydrogen-bonded network. Our data demonstrate that the shear mechanical spectra are able to reveal aspects of the relaxations dynamics in hydrogen-bonded materials which give no contribution to the dielectric signal.

II. Experiments

The glycerol–water mixtures were prepared using water from an Arium 611 ultrapure water system and glycerol from Sigma-Aldrich at 99.9% > purity. The concentrations used were x_{gly} = 1, 0.8, 0.7, 0.6, 0.5 and 0.3. Table 1 gives an overview of the precise concentrations used. For the measurement on neat glycerol the sample was loaded into the cell under nitrogen atmosphere in order to avoid uptake of water from the air.

The employed experimental method is the "piezoelectric shear-modulus gauge" (PSG) technique[41] covering the frequency range from mHz to kHz corresponding to timescales ranging from *ca.* 100 seconds to *ca.* 10 microseconds. The measured quantity is the complex frequency-dependent shear modulus $G^*(\nu) = G'(\nu) + iG''(\nu)$ defined for a harmonic oscillation stress and strain by

$$G^* = \frac{\sigma_0}{\gamma_0} e^{i\delta} \quad (1)$$

where σ_0 and γ_0 are the amplitudes of the stress and strain respectively and δ is the phase difference between stress and strain. The complex modulus has an imaginary part whenever $\delta \neq 0$. Data were measured upon cooling in the range from roughly 30 degrees above T_g down to T_g in steps of a couple of degrees.

Table 1 Overview of the concentrations used

$m_{glycerol}$	m_{water}	x_{gly}^{mol}	x_{gly}^{vol}	x_{gly}^{weight}
6.318	0	1	1	1
6.315	0.308	0.800	0.942	0.953
6.305	0.528	0.700	0.905	0.923
6.308	0.823	0.600	0.859	0.885
6.323	1.232	0.500	0.802	0.837
6.339	2.877	0.301	0.636	0.688

III. Results and analysis

A. Raw data and temperature dependence

In Fig. 1 we show the frequency dependence of the real and imaginary part of the shear modulus plotted on linear *y*-scales, for neat glycerol and two out of the five investigated mixtures. The real part of the shear modulus goes to zero at low frequencies indicative of the viscous flow, while it reaches a finite value at high frequencies, because the liquid behaves like a solid at short time scales. The transition between the viscous and the elastic behaviors gives rise to a peak in the imaginary part, commonly referred to as the loss peak. The loss peak shifts to lower frequencies as the liquid is cooled and the solid-like limiting behavior will fill the entire frequency range when the liquid reaches the glass transition temperature.

In Fig. 2(a) we show the evolution of the frequency of the loss peak maximum, ν_{max}, with temperature. In this representation it

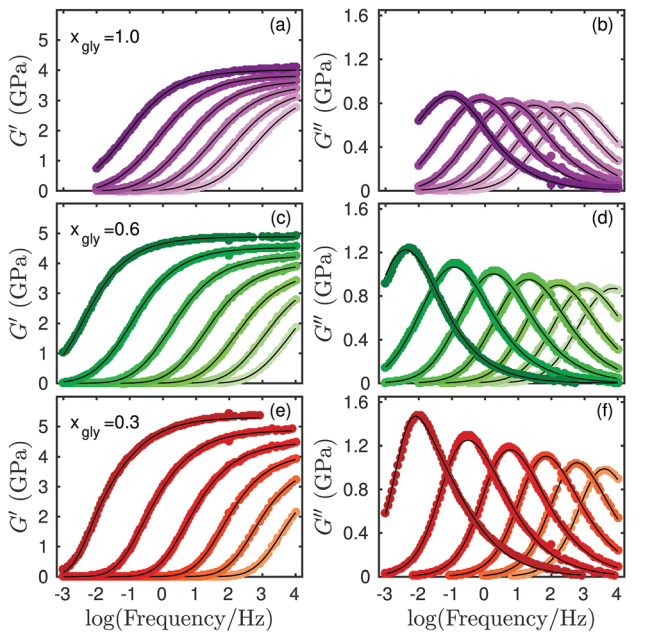

Fig. 1 The complex shear modulus for three of the six concentrations studied. Temperatures shown for x_{gly} = 1 range from 190 K to 210 K in step of 4 K, for x_{gly} = 0.6 from 175 K to 205 K in step of 5 K, and for x_{gly} = 0.3 from 165 K to 190 K in step of 5 K. The black lines are fits of the data to an extended Maxwell model presented in ref. 42. An example of the fits on a log–log scale is shown in Fig. 5(c).

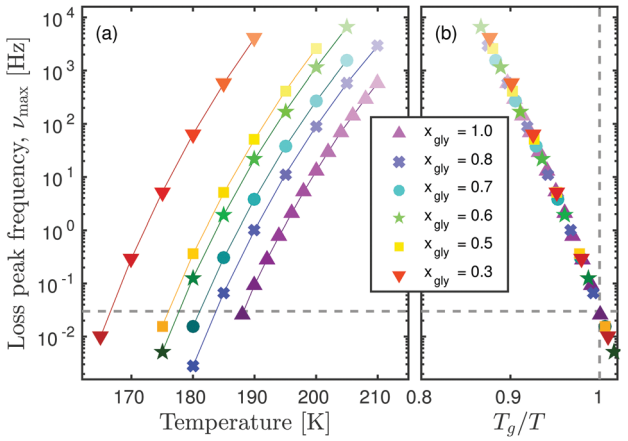

Fig. 2 Relaxation map for the investigated glycerol–water mixtures. (a) Loss peak frequencies as a function of temperature for the different concentrations. The plasticising effect of water lowers T_g and shifts the curves to lower temperature with increasing water content. (b) All curves collapse when plotted against inverse temperature scaled with T_g (defined as the $\nu_{max}(T_g)$ = 30 mHz and shown by the dashed line). Thus the temperature behavior of the relaxation time is surprisingly similar across the entire concentration range explored here.

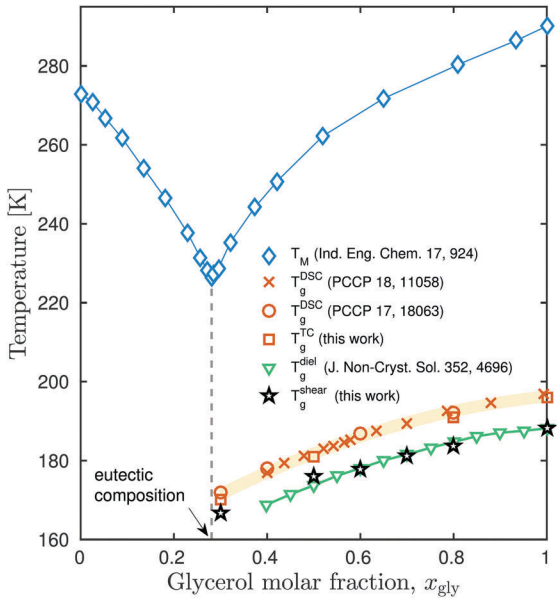

Fig. 3 The glass and melting transition temperatures as a function of glycerol concentration. The eutectic point occurs at X_{gly} = 0.28 (melting point data from ref. 46). Glass transition temperatures roughly obeys the 2/3 rule in the range of concentrations explored in this work (all above the eutectic composition). The T_g curves depend slightly on the method of determination: calorimetric curves – differential scanning calorimetry (DSC) and thermalization calorimetry (TC) – are higher than the dielectric and shear, but follow the same trend. DSC data are from ref. 14 and 47. Dielectric data are found in ref. 21, where the T_g is defined as $\tau(T_g) \equiv 100$ s. Shear data are from this work using T_g defined in Fig. 2. TC data are obtained by the method described in ref. 48.

becomes clear that adding water to glycerol has a plasticizing effect, as for a given temperature the loss peak frequency increases. This behavior is consistent with the dielectric measurements.[14,19] The water-induced increase in the overall molecular mobility render a lower glass transition temperature, T_g, in harmony with previous results obtained from differential scanning calorimetry performed on the same mixtures.[43] In the following we will introduce T_g^{shear} as the temperature at which the modulus loss peak frequency ν_{max} reaches 30 mHz. This frequency is chosen to avoid extrapolation and corresponds to a relaxation time of 5 seconds. Fig. 2(b) depicts the loss peak frequencies on a reduced temperature scale, where for each concentration the inverse temperature axis is multiplied by the corresponding value of T_g^{shear}. One can easily observe that such a scaling render a good overlap of all the data sets, disregarding the water concentration. In other words, the relative temperature dependence of the relaxation time, which can be quantified by the fragility index $m = d\log\tau/d(T_g/T)$,[44] is surprisingly unaffected by the addition of water.

Fig. 3 shows the phase diagram for glycerol–water mixtures. Here the T_g^{shear} obtained above are compared to T_g-data obtained *via* complementary techniques. One may note that the lowest glycerol concentration considered in the present study is close to the eutectic point of this mixture, which occurs at a glycerol molar concentration of x_{gly} = 0.28. In the investigated concentration range the decrease in T_g occurring upon lowering x_{gly} mirrors the depression of melting temperature, T_M, as the two characteristic temperatures comply well with the empiric proportionality $T_g/T_M \approx 2/3$.[45]

B. Spectral shape and slow mode

In order to study the variation of the spectral shape with water content we plot the data from Fig. 1 on a logarithmic scale, and normalized with respect to both the loss peak frequency, ν_{max}, and the amplitude of the signal.

This is shown in Fig. 4(a) and (b) which contain for clarity reasons a single spectrum for each investigated concentration. The corresponding temperature was chosen so that the relaxation time of the different mixtures roughly coincide. All spectra clearly exhibit at lowest frequencies the $G''(\nu) \propto \nu$ and $G'(\nu) \propto \nu^2$ power laws which are characteristic for viscous flow.[49] However, for the neat glycerol as well as for the mixtures with highest glycerol concentrations a low frequency shoulder can be identified in both the real and the imaginary parts before the viscous flow sets in. This spectral contribution which is slower than the structural (alpha) relaxation strongly resembles the mechanical mode which is discussed for monoalcohols in connection with the formation of hydrogen-bonded supramolecular structures.

To further strengthen this point, we have included for comparison the liquids 2-ethyl-1-hexanol (2E1H) and tetramethyltetraphenyl-trisiloxane (DC704) to Fig. 4(a) and (b). 2E1H is a paradigmatic monoalcohol which is known to exhibit a supramolecular relaxation clearly seen as a distinct slow mode in the mechanical spectra as well as a strong Debye signal in the dielectric spectra,[35] while DC704 is a van der Waals liquid with no additional modes and a "simple" behavior in general.[50,51] As observed in Fig. 4(a) and (b) the shape of the mechanical spectra of the glycerol–water mixtures fall between the spectra

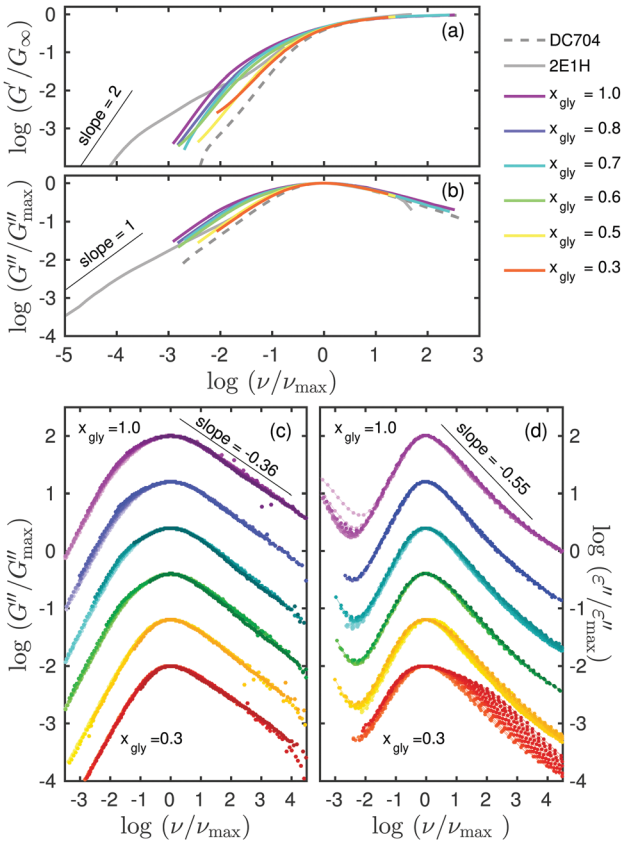

Fig. 4 The spectral shape of glycerol and its mixtures with water. (a and b) Real and imaginary part of the normalized shear modulus of a single spectrum for each concentration. For comparison we have added the liquids 2-ethyl-1-hexanol (2E1H) and tetramethyl-tetraphenyl-trisiloxane (DC704) (data from ref. 35 and 50). (c and d) Normalized TTS plots of the loss peak of all the shear spectra (this work) and the dielectric spectra (data from ref. 14). Each concentration has been given an offset to make comparison between the concentrations easier. Clearly, the spectral shapes in shear and dielectric are quite different (see also Fig. 6) as is their evolution with concentration.

of these two liquids, with neat glycerol being closer to 2E1H, while the glycerol–water mixtures resemble more DC704 with the increase of water content. Accordingly, neat glycerol behaves like a liquid with supramolecular structure dynamics while adding water makes it behave more like a liquid devoid of supramolecular associations.

In Fig. 4(c) and (d) we show the normalized imaginary part of all the shear spectra (this work) and the corresponding dielectric loss spectra (data from ref. 14). The scaled data are presented in arbitrary units as each concentration has been given an offset to make comparison of the concentrations easier. Clearly no low-frequency Debye mode is visible in the dielectric spectrum of glycerol nor any of the studied glycerol–water mixtures. Thus, whatever mechanism is responsible for the observed slow rheological mode is not giving rise to a net electric polarization. This is markedly different from the situation for monoalcohols where a strong dielectric signal emerges due to collective dynamics of the individual (molecular) dipoles.[25]

In order to quantify the degree of separation between the mechanically active slow mode and the alpha relaxation we introduce the classical Maxwell time given by:

$$\tau_M = \frac{\eta_0}{G_\infty} \quad (2)$$

where η_0 and G_∞ are given by the limiting behaviors:

$$\eta_0 \equiv \lim_{\omega\to 0}(G''(\omega)/\omega) \quad (3)$$

$$G_\infty \equiv \lim_{\omega\to\infty}(G'(\omega)). \quad (4)$$

In the simplest case, corresponding to exponential relaxation in the time domain, one has $2\pi\nu_{max}\tau_M = 1$. For van der Waals liquids this relation holds to a good approximation. On the other hand, the two time scales, $1/(2\pi\nu_{max})$ and τ_M, are separated by an order of magnitude for the monoalcohols displaying a clear signature of the polymer-like slow mode.[35] Thus $2\pi\nu_{max}\tau_M$ is a decoupling index and deviations from $2\pi\nu_{max}\tau_M = 1$ quantifies the separation of the two timescales. The Maxwell relaxation time, τ_M, corresponds to the slowest mode in this analysis. To determine τ_M one needs to experimentally reach the low-frequency terminal mode and to reliably estimate the high frequency plateau of the real part. Since we are restricted in our frequency window we can not resolve both limiting regimes for all temperatures. In practice, we obtain τ_M from the fits shown in Fig. 1. The model function has τ_M as one of the parameters and is able to describe the low-frequency mode in the data (illustrated in Fig. 5(c)).

In Fig. 5(a) the separation of the two relaxation times, defined as $\log(2\pi\nu_{max}\tau_M)$, is shown for all the investigated concentrations. For comparison we again show the results of the van der Waals bonded liquid DC704 and the monoalcohol 2E1H. The first observation is that the separation between the two time scales decreases with increasing water content. This becomes even clearer in Fig. 5(b) where the separation is shown as a function of concentration for $\nu_{max} = 10$ Hz (indicated by the dashed vertical line in Fig. 5(a)) determined by linear interpolation. There is a sudden increase in time-scale separation between $x_{gly} = 0.5$ and $x_{gly} = 0.6$ and very different trends with concentration in the regions below and above.

Another observation from Fig. 5(a), is that at concentrations from $x_{gly} = 0.6$ and above the time-scale separation appears to have a temperature dependence, with the separation increasing as the temperature decreases. In other words the time-temperature superposition (TTS) does not exactly hold for the dynamics slower than the alpha process, which can also be seen if one looks carefully at Fig. 4(c). A zoom of the neat glycerol data is depicted in Fig. 5(d) in order to show the deviation of TTS directly in the spectra. Below $x_{gly} = 0.6$ the decoupling index is constant or slightly decreasing with decreasing temperature.

If the spectral shapes were identical then all time scales would be proportional. However, Fig. 5 shows that this is not the case, and thus temperature and concentration dependencies will be affected by the choice of characteristic time scale. In Fig. 2 and 3 we have used the loss peak frequencies, because

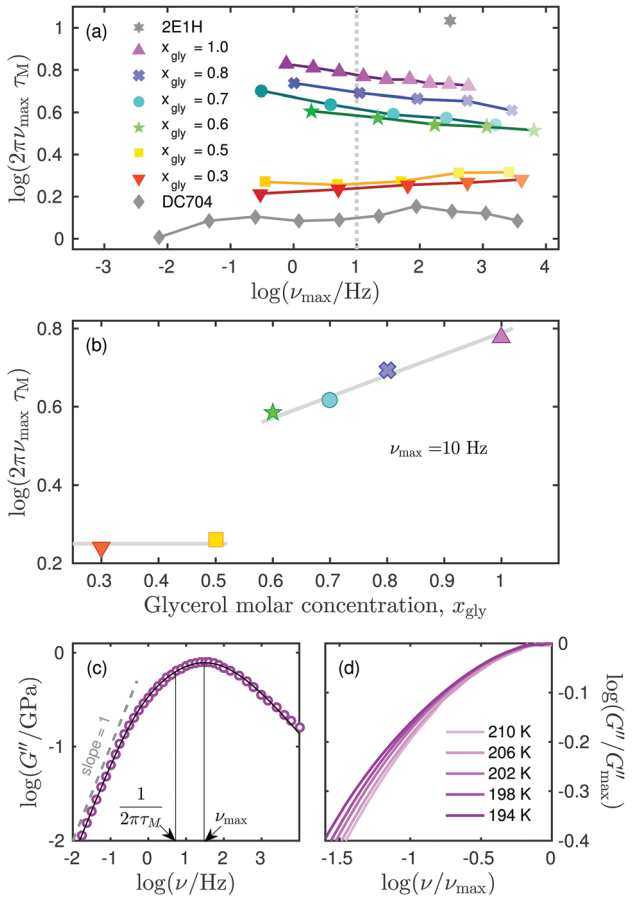

Fig. 5 Decoupling between the two timescales $1/(2\pi\nu_{max})$ and τ_M. (a) Decoupling index as a function of loss peak frequency. For $x_{gly} \geq 0.6$ the decoupling index decreases slightly with temperature. For $x_{gly} \leq 0.5$ it is constant or perhaps slightly increasing. For comparison the decoupling index of DC704 and 2E1H is shown. (b) The decoupling index evaluated at a loss peak frequency of 10 Hz (marked by the vertical dashed line in (a) and determined by linear interpolation) as a function of glycerol concentration. The index is increasing as a function of concentration with a dramatic change between x_{gly} = 0.5 and x_{gly} = 0.6. Lines are guides to the eye that highlight the different trends in the two regions. (c) Illustrating for a single neat glycerol spectrum the difference between the loss peak frequency and the fitted Maxwell time. Circles are data points, the full line is the fit. (d) Zoom of the neat glycerol curves in Fig. 4 showing the deviation from TTS.

this is a model independent measure of a characteristic time scale for the relaxation and accessible for most of the studied temperatures. If instead we would have used the Maxwell time, the curves of all concentrations $x_{gly} \geq 0.6$ in Fig. 2(a) would separate more from the two low concentrations and consequently the T_g^{shear} points in Fig. 3 would fall on a smoother curve.

C. High frequency behavior

Another interesting observation, arising when comparing the shear mechanical spectra to the dielectric ones, relates to the high frequency flank of the spectrum. The dielectric alpha relaxation peak of glycerol is often reported to be relatively narrow compared to van der Waals liquids, as the high frequency flank of the dielectric spectra is steeper.[52] However, in the shear

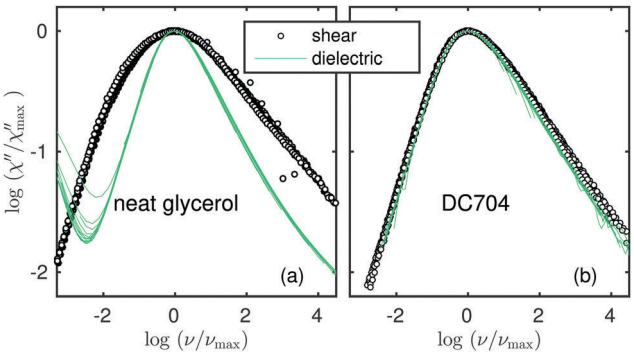

Fig. 6 Comparison of shear and dielectric spectral shapes for (a) neat glycerol and (b) DC704. For glycerol the spectral shapes are very different: the dielectric spectrum is narrow and steep while the shear mechanical spectrum is broad due to the low frequency shoulder and a less steep high frequency slope. In the case of DC704 the observation is the opposite; dielectric and shear mechanical spectra for DC704 are nearly indistinguishable. This shows that for some liquids different probing techniques reveal very different behavior.

modulus loss spectrum the high frequency slope in the double logarithmic plot is close to −0.4 indicating a rather broad underlying distribution of shear relaxation times.

These high-frequency power-law behaviors are sketched in Fig. 4(c) and (d). Note that the shear data in Fig. 4(c) and the dielectric data in Fig. 4(d) have the same scale on the frequency axis. It is obvious, that the two different response functions are characterized by different degrees of stretching. This is unlike the case for the van der Waals liquid DC704 where the dielectric and shear mechanical loss peaks are barely distinguishable when plotted in this normalized form.[50] This striking difference between glycerol and DC704 is depicted in Fig. 6.

As observed in Fig. 4(d) a second high frequency relaxation process becomes clearly visible for x_{gly} = 0.3 separating from the main relaxation peak with decreasing temperature. This mode is absent in the shear mechanical spectra, and thus has a completely different behavior from high frequency beta-relaxations in neat systems, which are usually more pronounced in the shear mechanical spectra than the dielectric spectra.[50,53,54]

IV. Discussion

A. Neat glycerol

The shear spectra of glycerol resolve an enhanced low frequency stiffness which is not present in non-associating molecular liquids. On the other hand, the spectral shape of its corresponding dielectric susceptibility lacks the complexity of monoalcohols. Could it be that in the case of glycerol one encounters slow dynamics which is rheologically, yet not dielectrically active? A similar behavior was reported by some of us for 2-ethyl-1-hexylamine,[38] and to address this question one has to understand in the first place what kind of structural foundation may support the emergence of the dielectric Debye mode. For monoalcohols a general agreement has been established that they form quasilinear supramolecular structures with the backbone formed by the hydrogen-bonded hydroxyl groups.[25]

Corroborating the magnitude of the dielectric strength with this kind of topology, one may rationalize that in monoalcohols the supramolecular clusters can occur as chains or rings, depending on steric hindrance of OH-groups. The *n*-alcohols with the OH-groups located at the extremity of the molecules are able to sustain moderately long chains. From the dielectric perspective these chains can be represented as ''end-to-end'' dipole moments resulting from the vector summation of the individual dipole moments along the backbone. The fluctuations of these mesoscopic dipoles are often considered to be the origin of the Debye mode which resemble to a certain extent the situation of dielectric normal modes in type A polymers.[55] Within these structural considerations one may understand why a similar dielectric Debye mode is not generated in glycerol: with the possibility of several hydrogen bonds per molecule, glycerol can form a branched network and thus any preference in the direction of local association vanishes and so does the effective dipole moment, contrary to the situation for monoalcohols.

Continuing with the analogy to polymeric behavior it is instructive to compare our results to the results of ref. 56 where the mechanical signature of a linear polymers is compared to that of dendrimers. While the linear polymers display a slow mode clearly separated from the alpha-relaxation and a distinct rubber plateau in the real part of the shear modulus, the dendrimers only display reminiscence of the Rouse dynamics in terms of a low frequency shoulder on the mechanical loss peak. The difference in the mechanical spectrum of monoalcohols and glycerol mimics the behavior seen for linear polymers and dendrimers depicted in Fig. 4 of ref. 56. The monoalcohol exhibits a clearly separated mode as does the linear polymer, while in glycerol there is only a shoulder as was the case for dendrimers. This observation supports the interpretation above, namely that the slow mode and the dielectric Debye-signal in monoalcohols are due to dynamics associated with a linear structure formed by hydrogen-bonds, while the slow mode in glycerol is associated with the branched hydrogen-bonded structures.

B. Glycerol–water mixtures

The slow polymer-like rheological mode which we observe in glycerol decreases in significance as water is added and effectively dies out at equimolar composition. Under the assumption that the slow mode is due to dynamics of supramolecular hydrogen-bonded structures as argued above, this would imply that water drastically changes the hydrogen-bonded structures and/or their dynamics.

There are several works in the literature on the structure of water–glycerol mixtures, and though most of these studies are carried out at or close to room temperature we will use these to guide our interpretation of our findings.

Maybe the most basic structural finding from literature is that the glycerol–water mixtures have a negative excess molar volume,[57] which means that the total volume decreases upon mixing. The excess molar volume has a minimum close to $x_{gly} \approx 0.3$ coinciding with the minimum in the melting transition temperature (Fig. 3). The negative excess molar volume indicates that there is an increased packing efficiency as the water concentration increases in the range studied in this work. Moreover, it has been shown that the internal structure of glycerol itself changes when mixed with water,[58] which might also have a direct effect on the molecular packing efficiency.

Towey *et al.* used neutron scattering in combination with Reverse Monte Carlo (RMC) simulations to study the hydrogen-bonded structure in glycerol[59] as well as in glycerol–water mixtures.[60–63] They find that in neat glycerol each molecule forms on average 5.68 ± 1.51 hydrogen bonds, while for neat water the average number of hydrogen bonds per molecule is about 3.56 ± 1.10. Mixing water and glycerol preserves to a large extent the number of hydrogen bonds per molecule although the number of glycerol–glycerol hydrogen bonds decreases progressively as they are replaced by glycerol–water bonds, so the hydrogen-bonded structure changes.

We assume that the changes we see in the mechanical spectra among the different compositions must be due to changes in the dynamics of the concentration dependent hydrogen-bonded network. The sudden change at glycerol concentration $0.5 < X_{gly} < 0.6$ suggests a qualitative change of the network behavior around this concentration. Indeed, in ref. 63 Towey *et al.* studied the cluster size distribution and revealed that percolating water clusters are found at mole fractions $x_{gly} = 0.5$ and below, while percolating glycerol clusters are found from $x_{gly} = 0.25$ and above. As mentioned above, one should be careful when comparing our findings to the results of Towey *et al.* which are obtained with the aid of RMC and data taken at room temperature, while we study deeply supercooled samples. Nevertheless, it is striking that the concentration $x_{gly} \simeq 0.5$ where we observe a dynamical change coincides with a structural change for the water clusters in terms of percolation, while nothing dramatic happens to the glycerol–glycerol network. An interpretation could be that water acts as a ''lubricant'', reducing the low frequency stiffness of the glycerol network.

In ref. 22 it is noted that the dielectric spectra obey time temperature superposition for glycerol concentrations above 0.55 while this superposition breaks down at $x_{gly} = 0.55$, and a clear high frequency mode appears when the glycerol concentration is below $x_{gly} = 0.4$. It is tempting to ascribe this fast dynamics to a Johari–Goldstein beta-process which is generally exhibited by neat glass-forming systems near their glassy state. However, this high frequency spectral contribution is absent in the complementary shear mechanical spectra. Since the beta-relaxation generally is more pronounced in the mechanical spectra than in the dielectric ones,[50,53,54] it becomes clear that this water-induced relaxation mode cannot be regarded as a ubiquitous secondary process. Instead, it has been suggested that the high frequency dielectric shoulder is a signature of water–water dynamics in aggregated water domains.[22]

In general hydrogen bonding is known as a driving force for clustering in water–alcohol mixtures and responsible of the limit of miscibility;[64] compared to these studies in the low viscosity (high T) regime, the effect of decreasing temperature

will be to enhance the phase separation. As the water concentration is increased we expect that there are increasing concentration fluctuations, and nano-segregation is likely to occur close to T_g in the mixtures with high water concentrations. Further structural investigations need to be considered for the elucidation of this peculiar mixing behavior and its connection with other anomalies of water-related materials.

V. Conclusion

In this work we demonstrate the existence of a slow rheological mode in neat glycerol. The slow relaxation feature is similar to the suprasegmental dynamics seen in dendrimers and we attribute it to the rearrangements of the branched hydrogen-bonded network. To our knowledge this is the first indication of hydrogen-bonded network dynamics in a poly-alcohol, while similar signals have been reported so far in monoalcohols only. However, no direct link between structure and dynamics is made in the present study and simultaneous experiments are highly desirable in the future.

The observed slow mode becomes weaker when adding water, and disappears quite abruptly at equimolar composition. This corresponds to the water concentration where percolating water clusters appear according to RMC simulations of neutron scattering data. We speculate that water acts as a lubricant softening the modes of the glycerol–glycerol hydrogen-bonded matrix. Further computer simulations could be helpful in this respect. Our results underlines how different parts of the dynamics in hydrogen-bonded systems are evident from different types of spectroscopy making the combination of complementary techniques imperative in this field.

Conflicts of interest

There are no conflicts to declare.

Acknowledgements

We thank Ivan Popov and Prof. Yuri Feldmann for making the dielectric data of ref. 14 available in electronic form. The following funding bodies are acknowledged: Danish Council for Independent Research (Sapere Aude: Starting Grant), the Danish National Research Foundation (DNRF61) and Laboratoire Léon Brillouin (UMR CEA-CNRS, Paris-Saclay).

References

1 L. Pauling, *The Nature of the Chemical Bond and The Structure of Molecules and Crystals*, Cornell University Press, Ithaca, NY, 1939.
2 G. A. Jeffrey and W. Saenger, *Hydrogen Bonding in Biological Structures*, Springer-Verlag, Berlin, 1991.
3 G. R. Desiraju and T. Steiner, *The Weak Hydrogen Bond in Structural Chemistry and Biology*, Oxford University Press, Chichester, 1999.
4 Y. Maréchal, *The hydrogen bond and the water molecule: The physics and chemistry of water, aqueous and bio-media*, Elsevier, Amsterdam, 2007.
5 G. E. Gibson and W. F. Giauque, *J. Am. Chem. Soc.*, 1923, **45**, 93.
6 C. H. Wang and R. B. Wright, *J. Chem. Phys.*, 1971, **55**, 1617.
7 B. Schiener, R. Böhmer, A. Loidl and R. Chamberlin, *Science*, 1996, **274**, 752.
8 L. Berthier, G. Biroli, J.-P. Bouchaud, L. Cipelletti, D. E. Masri, D. L'Hôte, F. Ladieu and M. Pierno, *Science*, 2005, **310**, 1797.
9 T. Pezeril, C. Klieber, S. Andrieu and K. A. Nelson, *Phys. Rev. Lett.*, 2009, **102**, 107402.
10 S. Albert, T. Bauer, M. Michl, G. Biroli, J.-P. Bouchaud, A. Loidl, P. Lunkenheimer, R. Tourbot, C. Wiertel-Gasquet and F. Ladieu, *Science*, 2016, **352**, 1308.
11 R. W. Salt, *Nature*, 1958, **181**, 1281.
12 J. L. Dashnau, N. V. Nucci, K. A. Sharp and J. M. Vanderkooi, *J. Phys. Chem. B*, 2006, **110**, 13670.
13 D.-X. Li, B.-L. Liu, Y. Shu Liu and C. Lung Chen, *Cryobiology*, 2008, **56**, 114.
14 I. Popov, A. G. Gutina, A. P. Sokolov and Y. Feldman, *Phys. Chem. Chem. Phys.*, 2015, **17**, 1.
15 K.-i. Murata and H. Tanaka, *Nat. Mater.*, 2012, **11**, 436.
16 P. Lunkenheimer, U. Schneider, R. Brand and A. Loid, *Contemp. Phys.*, 2000, **41**, 15.
17 C. Gainaru, A. Rivera, S. Putselyk, G. Eska and E. A. Rössler, *Phys. Rev. B: Condens. Matter Mater. Phys.*, 2005, **72**, 174203.
18 S. Sudo, M. Shimomura, N. Shinyashiki and S. Yagihara, *J. Non-Cryst. Solids*, 2002, **307-310**, 356.
19 A. Puzenko, Y. Hayashi, Y. E. Ryabov, I. Balin, Y. Feldman, U. Kaatze and R. Behrends, *J. Phys. Chem. B*, 2005, **109**, 6031.
20 A. Puzenko, Y. Hayashi and Y. Feldman, *J. Non-Cryst. Solids*, 2007, **353**, 4518.
21 Y. Hayashi, A. Puzenko, I. Balin, Y. E. Ryabov and Y. Feldman, *J. Phys. Chem. B*, 2005, **109**, 9174.
22 Y. Hayashi, A. Puzenko and Y. Feldman, *J. Non-Cryst. Solids*, 2006, **352**, 4696.
23 S. S. N. Murthy and S. K. Nayak, *J. Chem. Phys.*, 1993, **99**, 5362.
24 H. Huth, L.-M. Wang, C. Schick and R. Richert, *J. Chem. Phys.*, 2007, **126**, 104503.
25 R. Böhmer, C. Gainaru and R. Richert, *Phys. Rep.*, 2014, **545**, 125.
26 L. P. Singh, C. Alba-Simionesco and R. Richert, *J. Chem. Phys.*, 2013, **139**, 144503.
27 D. Morineau and C. Alba-Simionesco, *J. Chem. Phys.*, 1998, **109**, 8494.
28 A. Mandanici, M. Cutroni and R. Richert, *J. Chem. Phys.*, 2005, **122**, 084508.
29 Y. Gao, D. Bi, X. Li, R. Liu, Y. Tian and L.-M. Wang, *J. Chem. Phys.*, 2013, **139**, 024503.
30 L.-M. Wang and R. Richert, *J. Chem. Phys.*, 2005, **123**, 054516.
31 T. Cosby, A. Holt, P. J. Griffin, Y. Wang and J. Sangoro, *J. Phys. Chem. Lett.*, 2015, **6**, 3961.
32 K. Adrjanowicz, K. Kaminski, M. Dulski, P. Wlodarczyk, G. Bartkowiak, L. Popenda, S. Jurga, J. Kujawski, J. Kruk and M. K. Bernard, *et al.*, *J. Chem. Phys.*, 2013, **139**, 111103.

33 M. Rams-Baron, Z. Wojnarowska, M. Dulski, A. Ratuszna and M. Paluch, *Phys. Rev. E: Stat., Nonlinear, Soft Matter Phys.*, 2015, **92**, 022309.
34 S. Pawlus, S. Klotz and M. Paluch, *Phys. Rev. Lett.*, 2013, **110**, 173004.
35 C. Gainaru, R. Figuli, T. Hecksher, B. Jakobsen, J. C. Dyre, M. Wilhelm and R. Böhmer, *Phys. Rev. Lett.*, 2014, **112**, 098301.
36 T. Hecksher, *J. Chem. Phys.*, 2016, **144**, 161103.
37 J. D. Ferry, *Viscoelastic Properties of Polymers*, Wiley, New York, 1980.
38 K. Adrjanowicz, B. Jakobsen, T. Hecksher, K. Kaminski, M. Dulski, M. Paluch and K. Niss, *J. Chem. Phys.*, 2015, **143**, 181102.
39 T. Cosby, Z. Vicars, Y. Wang and J. Sangoro, *J. Phys. Chem. Lett.*, 2017, **8**, 3544.
40 T. Hecksher and B. Jakobsen, *J. Chem. Phys.*, 2014, **141**, 101104.
41 T. Christensen and N. B. Olsen, *Rev. Sci. Instrum.*, 1995, **66**, 5019.
42 T. Hecksher, N. B. Olsen and J. C. Dyre, *J. Chem. Phys.*, 2017, **146**, 154504.
43 Physical Properties of Glycerine and Its Solutions (Glycerine Producers' Association, 1963).
44 C. A. Angell, *J. Non-Cryst. Solids*, 1991, **131**, 13.
45 E.-J. Donth, *The Glass Transition: Relaxation Dynamics in Liquids and Disordered Materials*, Springer Series in Materials Science, Springer, 2001, vol. 48.
46 L. Lane, *Ind. Eng. Chem.*, 1925, **17**, 924.
47 J. Bachler, V. Fuentes-Landete, D. A. Jahn, J. Wong, N. Giovambattista and T. Loerting, *Phys. Chem. Chem. Phys.*, 2016, **18**, 11058.
48 B. Jakobsen, A. Sanz, K. Niss, T. Hecksher, I. H. Pedersen, T. Rasmussen, T. Christensen, N. B. Olsen and J. C. Dyre, *AIP Adv.*, 2016, **6**, 055019.
49 G. Harrison, *The Dynamic Properties of Supercooled Liquids*, Academic press (INC.) London LTD, 1976.
50 B. Jakobsen, K. Niss and N. B. Olsen, *J. Chem. Phys.*, 2005, **123**, 234511.
51 L. A. Roed, K. Niss and B. Jakobsen, *J. Chem. Phys.*, 2015, **143**, 221101.
52 R. Böhmer, K. L. Ngai, C. A. Angell and D. J. Plazek, *J. Chem. Phys.*, 1993, **99**, 4201.
53 K. Niss, B. Jakobsen and N. B. Olsen, *J. Chem. Phys.*, 2005, **123**, 234510.
54 B. Jakobsen, K. Niss, C. Maggi, N. B. Olsen, T. Christensen and J. C. Dyre, *J. Non-Cryst. Solids*, 2011, **357**, 267.
55 *Broadband dielectric spectroscopy*, ed. F. Kremer and A. Schönhals, Springer, Berlin, 2003.
56 M. Hofmann, C. Gainaru, B. Cetinkaya, R. Valiullin, N. Fatkullin and E. A. Rössler, *Macromolecules*, 2015, **48**, 7521.
57 G. I. Egorov, D. M. Makarov and A. M. Kolker, *Thermochim. Acta*, 2013, **570**, 16.
58 A. V. Egorov, A. P. Lyubartsev and A. Laaksonen, *J. Phys. Chem. B*, 2011, **115**, 14572.
59 J. J. Towey, A. K. Soper and L. Dougan, *Phys. Chem. Chem. Phys.*, 2011, **13**, 9397.
60 J. J. Towey, A. K. Soper and L. Dougan, *J. Phys. Chem. B*, 2011, **115**, 7799.
61 J. J. Towey and L. Dougan, *J. Phys. Chem. B*, 2012, **116**, 1633.
62 J. J. Towey, A. K. Soper and L. Dougan, *J. Phys. Chem. B*, 2012, **116**, 13898.
63 J. J. Towey, A. K. Soper and L. Dougan, *Faraday Discuss.*, 2013, **167**, 159.
64 P. A. Artola, A. Raihane, C. Crauste-Thibierge, D. Merlet, M. Emo, C. Alba-Simionesco and B. Rousseau, *J. Phys. Chem. B*, 2013, **117**, 9718.
65 For discussion and further references on the structure factors of monoalcohols, we refer to the review of Böhmer *et al.*[25].